Critical Review Vol. CR43, Optomechanical Design, ed. P.R. Yoder, Jr. (July 1992) Copyright SPIE

Advanced considerations of the lens-to-mount interface

Paul R. Yoder, Jr.

Consultant in Optical Engineering
1220 Foxboro Drive, Norwalk, Connecticut 06851

ABSTRACT

The most frequently used lens-to-mount interfaces involve direct contact of shaped shoulders, spacers and/or retainers onto the polished lens surfaces or onto ground bevels. In some cases, the lens rim may contact a machined surface of the mount. Elastomeric suspension of the lens in the mount is a possible alternative design. Surface-contact mount types reviewed here include "sharp corner", tangent and toroidal interface versions using retaining rings to hold the lenses against shoulders or spacers. Means for conservatively estimating stress build-up with-in the lens due to axial preload at assembly and at extreme temperatures are suggested. Examples showing the influences of different material characteristics (such as coefficients of thermal expansion and Young's modulus) and of both positive and negative changes of temperature from that existing at assembly are discussed.

1. INTRODUCTION

A reliable lens-to-mount interface design should constrain the lens throughout the survival temperature range and under all anticipated shock and vibration loadings without inducing potentially damaging amounts of stress into the optical or mechanical materials. Under operating conditions, changes in surface locations and orientations should conform to the allowable decentration, despace and tilt budgets while the stresses should result in acceptable levels of surface deformations and induced birefringence. As discussed elsewhere during this conference,[1] costs of the parts and of the labor needed to assemble and align the optics are also important factors to be considered during the design process. These are frequently influenced by the optomechanical interface design.

In this paper, we describe some of the more successful types of optomechanical interfaces for rotationally symmetric optics such as lenses and windows and we review approximate analytical methods used to assess the suitability of these alternative designs. These methods are then

illustrated with specific examples to show the influences of key design and material parameters. While the treatment of forces and stresses given here is somewhat simplistic, it can be used to compare alternate designs or to assess the need for experimental verification or for more rigorous analyses using, for example, finite element analysis methods.

Although we refer here to the optical parts as though they are always lenses made of glass and to mechanical parts (housings, cells, spacers, retainers, etc) as if they are always made of metal, it should be understood that many of these mounting considerations also apply to windows or filters or to rotationally-symmetric mirrors and to other materials such as plastics or crystals.

A force acting in the axial direction exerted by the mount onto the component is called axial preload. Frequently, a modest axial preload is created at assembly since this tends to prevent motion of the component relative to the mount under external forces such as acceleration. Forces exerted in the radial direction at the rim of the component are sometimes referred to as "hoop" forces. Both types of compressive forces tend to introduce stress into the glass and into the mount so should be kept within acceptable limits.

A glass lens can usually withstand compressive stress as large as $3.45X10^8$ N/m^2 without failure so this value is generally accepted as a "rule-of-thumb" survival tolerance.[2] In some designs, lens surfaces can be placed in tension as a result of applied forces. A commonly accepted tolerance for tensile stress is $6.9X10^6$ N/m^2. Under operating environmental conditions, distortions of optical surfaces due to mounting stresses can degrade performance. No simple means for predicting refracting or reflecting surface deformations due to external forces are currently available. Techniques such as finite element analysis are usually employed to evaluate such deformations. Systems using polarized light may be sensitive to stress-induced birefringence within the refracting material. A "rule-of-thumb" tolerance for stress in such cases is $3.45X10^6$ N/m^2.

2. TYPICAL INTERFACE CONFIGURATIONS

The most frequently used lens-to-mount designs involve axial contact between annular areas on the mount and on the polished lens surfaces or on bevels ground into those surfaces. Radial contact between the rim of the lens and

the inside diameter (ID) of the mount also may occur. The stresses within the materials depend upon the geometric shapes of the contacting surfaces, the forces driving the surfaces together and the elastic properties of the materials used.

Use of a threaded retaining ring to secure a lens against a reference surface such as a shoulder or a spacer within a cell or housing offers advantages over other types of lens mounts in that this type mount can easily be assembled and disassembled without damage, it automatically compensates for lens edge thickness variations, it can provide a reasonably predictable axial preload and it is compatible with sealing with an injected sealant or with an O-ring.

Figures 1 through 4 illustrate concepts for interfaces between a cell shoulder, a lens and a threaded retainer. The simplest provides line contact at a "sharp corner" around the periphery of each lens surface. As shown in Fig. 1, this corner can be a 90° intersection between a cylindrical hole and a plane or an obtuse angle such as a 135° intersection between a conical hole and a plane. Acute corner angles should be avoided. A "sharp corner" interface can be used with either convex or concave lens surfaces. Accuracy of the actual intersection angle is not essential; errors of $\pm 2°$ usually are tolerable.

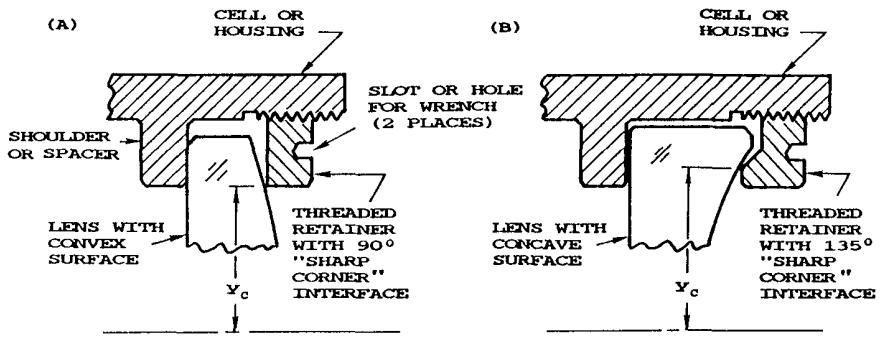

Fig. 1 - Concepts for "sharp corner" interfaces on (A) convex and (B) concave surfaces.

Good machining practice calls for the "sharp corner" to be burnished slightly to minimize burrs or nicks. Typically, a radius of the order of 0.05 mm then results.[3] A

tendency for better (i.e., smoother) sharp edges to result from machining an obtuse angle intersection was reported by Hopkins.[4] The radial height of line contact, y_c, usually is just slightly greater than the radius of the lens' clear aperture.

Tangential contact at a height y_c, is illustrated in Fig. 2. It can be used only with convex lens surfaces. The half-angle, φ, of the right-circular cone in such an interface is given by the following equation:

$$\varphi = 90° - \text{arc sin } (y_c/R) \qquad (1)$$

where R is the surface radius of curvature and y_c is typically one-half the arithmetic average of the lens' clear aperture and its OD. The typical tolerance on φ is $\pm 2°$.

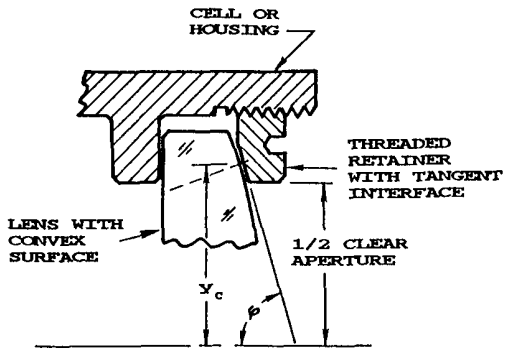

Fig. 2 - Concept for tangent interface on a convex surface.

Toroidal contact between the mechanical and optical components can be provided for either convex or concave lens surfaces. See Fig. 3. In each case, the center of curvature of the circular arc defining the "donut" is located off the axis by the dimension y_T and lies on the local normal to the lens surface passing through a point at height y_c defined as for tangent contact. Preferred values for the sectional radius of the toroids are 10R for a convex surface and 0.5R for a concave surface, where R is the radius of the lens surface.[5]

If the mechanical interface with the lens is lapped to the same spherical radius as the lens surface within a few

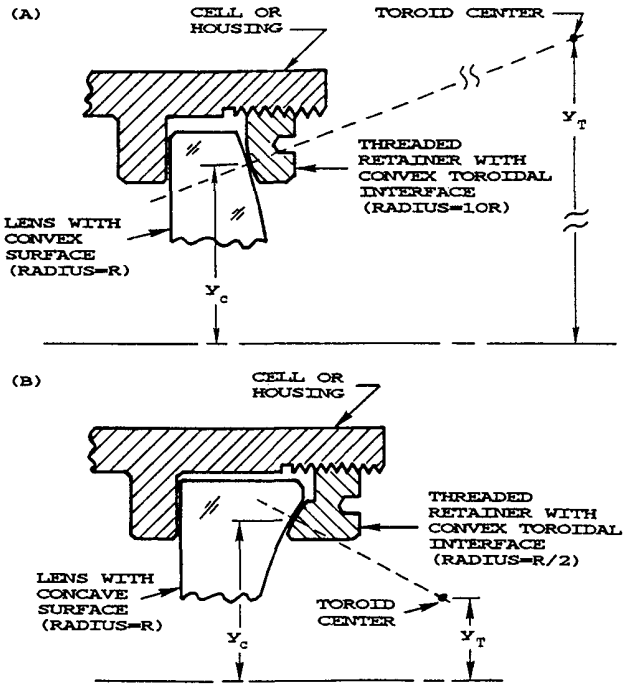

Fig. 3 - Concepts for toroidal interfaces on (A) convex and (B) concave surfaces.

fringes of visible light, a spherical interface mount can be produced. See Fig. 4. If the radii of the mechanical and optical surfaces do not match adequately, the interface will degenerate into line contact at the inner or outer edge of the annular mechanical area. Manufacture of the spherical interface mount is costly due to this need for radius matching. Hence, it is generally used only in special designs.

In each of the above described lens mounts, contact of the metal occurs on polished glass surfaces. These surfaces are usually accurately made and well aligned to each other due to the inherent nature of the optical grinding and edging processes. In most lenses, contact occurs at a zone where the optical surface is inclined with respect to the axially-directed force imposed by the retainer. Radial components of that force tend to center the lens with respect to the axis. The magnitude of this centering tendency depends upon the radius of curvature of the lens surface with sharply curved surfaces centering more easily.

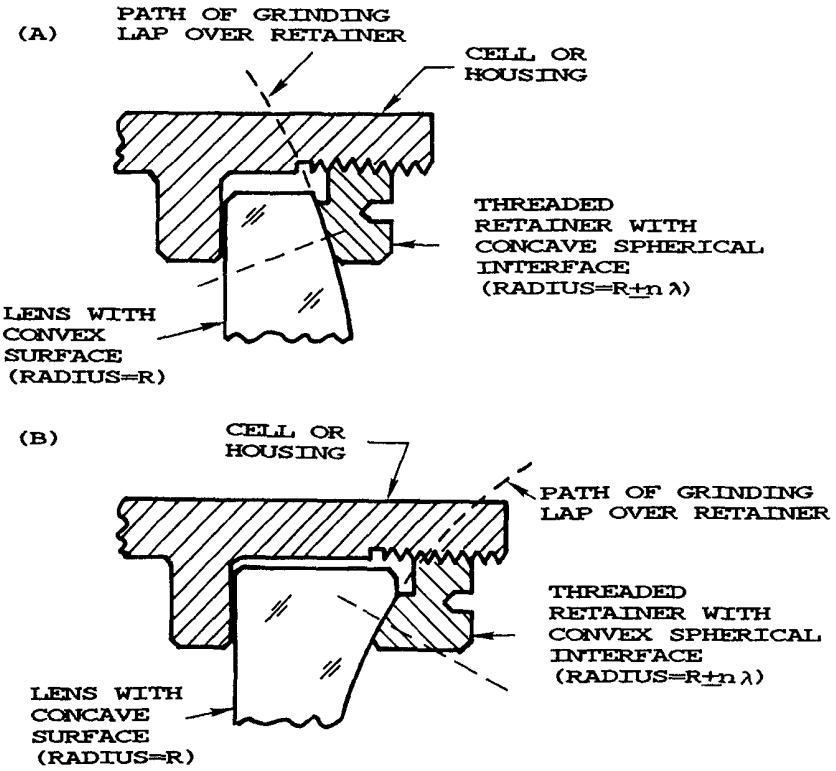

Fig. 4 - Concepts for spherical interfaces on (A) convex and (B) concave surfaces.

Contact against flat bevels ground into the edges of the lens' spherical surfaces can be provided as shown in Fig. 5. Such interfaces have the advantage of distributing axial preload due to the clamping action of the retaining ring over a large area on the lens thereby reducing stress build-up within the glass. They have the disadvantages of not being able to help self-center the lens and of referencing against secondary surfaces of potentially reduced angular accuracy as compared to the polished lens surfaces. While accurate flat bevels can be produced, they add significantly to the cost of the lens.

Resilient materials such as room temperature vulcanizing (RTV) elastomers are frequently used to seal optical components into their mounts with or without hard mechanical constraint. The resilient layer can provide some degree of protection against shock and vibration as well as some thermal isolation. Epoxy or urethane compounds are

sometimes used for the same purpose. These materials are generally somewhat less resilient than RTV compounds, but they are superior in regard to structural bond strength.

Figure 6 illustrates a common technique for mounting a lens in an annular ring of elastomer. Registry of one optical surface against a machined surface of the mount helps align the optic. Centration can be retained by temporary shimming or external fixturing

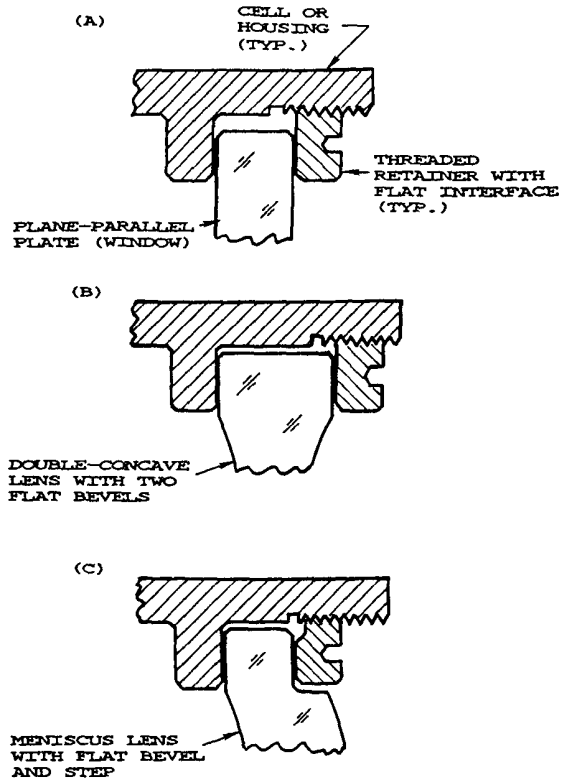

Fig. 5 - Concepts for flat bevel interfaces on (A) plano, (B) convex and (C) concave surfaces.

during the curing process. If the elastomer layer's radial thickness (t_E in the figure) is in accordance with an equation given in Section 4.5, the design becomes relatively insensitive to temperature changes.

3. AXIAL PRELOAD AND AXIAL STRESS EFFECTS

3.1 Effects at Assembly Temperature

If the optic is expected to experience acceleration

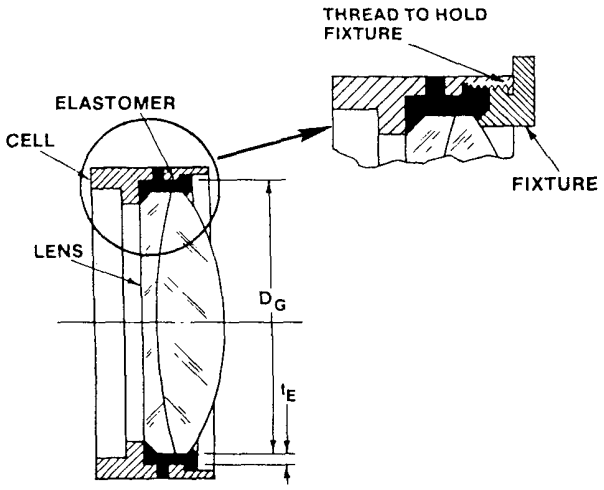

Fig. 6 - Concept for mounting a lens with an annular ring of elastomer. From Yoder.[11]

forces due to gravity, shock or vibration and its axial location within the mount must be held constant during such exposure by the axial force exerted by the retainer, it should be constrained by an axial preload, P_1, as given by the following equation:

$$P_1 = 9.807WA \qquad (2)$$

where:
P_1 is in newtons (N)
W = weight of optical component in kg
A = maximum imposed acceleration factor.

An additional amount of axial preload, P_2, might also be imposed upon the lens at assembly to ensure that the mount does not lose axial contact with the surface if it expands more than the glass as the temperature rises. This preload is discussed in Section 3.3.

If the glass and metal were inelastic, the contact would be along a line reaching around the perimeter of the lens surface at a radius y_c from the axis. Actually, both materials are somewhat elastic and deform slightly under pressure so contact occurs over a rectangular area of width Δy and length $2\pi y_c$. The magnitudes of Δy and of the contact area both vary by the square root of the preload. Large stresses can be created in the glass at the interface between the lens and the mount if the axial force is exerted upon a small area.

If we know the total preload, $P_T = P_1+P_2$, exerted by the retainer against the lens at the zonal contact radius, y_c, during assembly at a temperature of (typically) 20°C, the resulting peak axial stress, S_A, developed within the contact area can be estimated using the following equation from Rourk[6] as explained by Delgado and Hallinan[3] and by Yoder[5]:

$$S_A = 0.798(K_1 p/K_2)^{0.5} \qquad (3)$$

where:

S_A is in N/m^2

p = linear preload $= P_T/(2\pi y_c)$ in N/mm applied at the line contact near the rim of the lens

y_c = contact height in mm

$K_1 = (D_1+D_2)/D_1D_2$ for a sharp corner contacting a convex surface

$= (D_1-D_2)/D_1D_2$ for a sharp corner contacting a concave surface

$= 1/D_1$ for a conical surface contacting a convex surface (tangent interface)

$= 1.1/D_1$ for a toroid surface of sectional radius $10D_1$ contacting a convex surface

$= 1/D_1$ for a toroid surface of sectional radius $0.5D_1$ contacting a concave surface

D_1 = twice the lens radius of curvature in mm

D_2 = twice the sharp corner radius (typically 0.1 mm)

$K_2 = ((1-\nu_G^2)/E_G)+((1-\nu_M^2)/E_M)$

ν_G = Poisson's ratio for the glass

ν_M = Poisson's ratio for the metal

E_G = Young's modulus for the glass in N/m^2

E_M = Young's modulus for the metal in N/m^2.

Equations for the contact stresses introduced into a lens with flat bevel or spherical interfaces are not included here because those stresses would be relatively insignificant as compared to those with the interfaces listed. Typically, those stresses would equal the total preload divided by the area of contact. For "sharp corner" interfaces, D_2 is so small compared to the radius of most surfaces contacted, the values for K_1 (and hence contact stresses) are essentially the same for convex and concave surfaces. We noted earlier that tangential contact can occur only on convex surfaces. As shown by Yoder,[5] the stresses computed for both toroidal interface cases would be within five percent of those computed for the tangential case and much smaller than those for "sharp corner" interfaces.

Another equation from Rourk[6] can be used to estimate the annular width of the contact area between the elastically deformed surfaces. This is:

$$\Delta y = C(p)^{0.5} \qquad (4)$$

where

$$C = 1.6(K_2/K_1)^{0.5}$$

and all other terms are as defined above. The contact area is $2\pi y_c$ times this width.

As shown by Yoder,[7] the axial preload divided by the contact area is an average contact stress which must be multiplied by 1.2768 to give the peak axial stress as computed by Eq. (3).

3.2 Effects at Reduced Temperatures

When the temperature decreases by ΔT from that existing at assembly, the preload exerted by the retaining ring increases by P_3 due to differential contraction of the cell and the lens if the thermal expansion coefficient of the metal α_M exceeds that of the glass, α_G. P_T will then equal $P_1+P_2+P_3$. The contact stress within the glass, S_A' at the lower temperature depends upon the magnitude of this increased preload and can be computed by Eq. (3). The thermally-induced preload depends, in part, upon the cross-sectional areas within the mount and deep within the lens to which that force is applied. With the able help of Alson Hatheway[8] and Ralph Richard[9], the following approach has been developed for estimating these areas and the resultant thermally-induced preload.

Figure 7 shows the geometry of a typical lens cell. The wall thickness around the lens, the inner radius of this wall and the radius to the center of the cross-sectional area are indicated. This area is

$$A_M = 2\pi t_c((D_M/2)+(t_c/2)). \qquad (5)$$

Two cases for the geometry defining the affected area within the lens are shown in Fig. 8. The lens is assumed to be clamped between line contacts at radius y_c. The dashed lines form squares so, to reasonable approximation, the stress is limited to the shaded zone of annular width equal to the thickness t_E of the glass at y_c. For the case of Fig. 8(A), this zone lies within the lens and the area is given by Eq. (6).

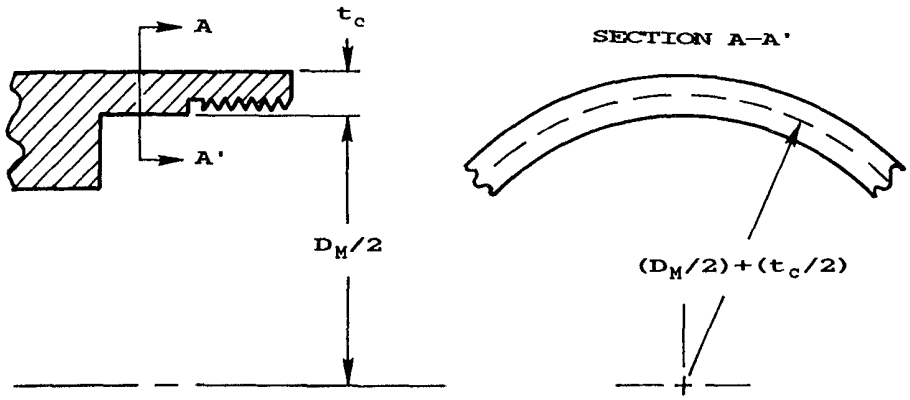

Fig. 7 - Geometric relationships determining the cross-sectional area of a lens cell wall.

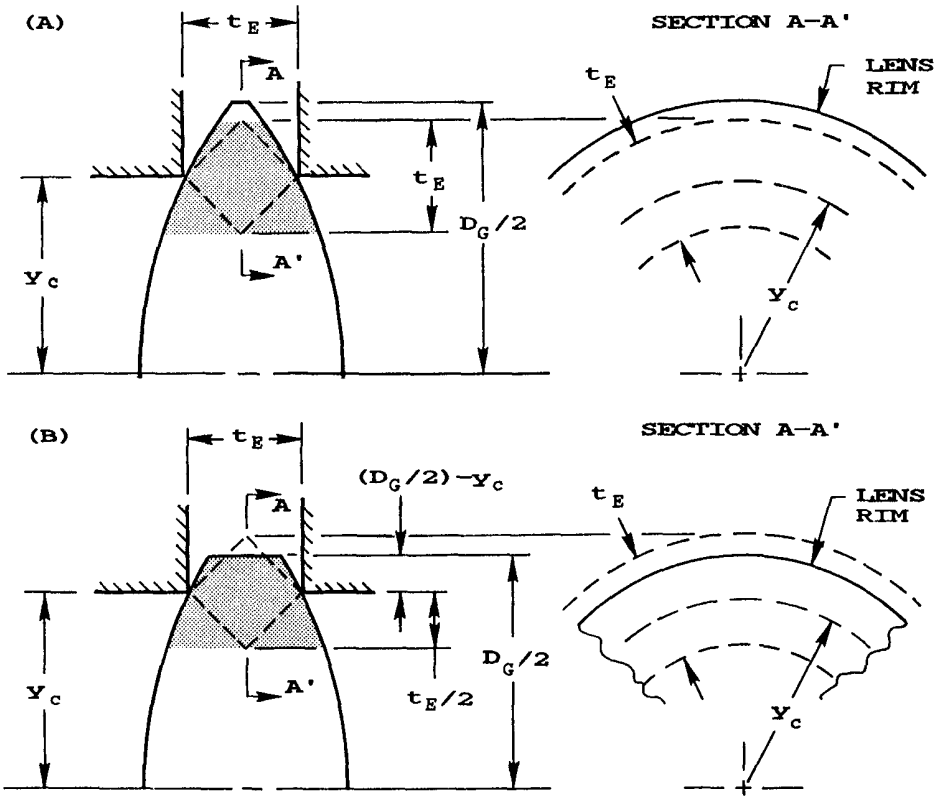

Fig. 8 - Geometric relationships determining the cross-sectional area of the stressed region within a clamped lens; (A) when this region lies within the lens rim and (B) when this region is truncated by the lens rim.

$$A_G = 2\pi y_c t_E . \quad (6)$$

If the line of contact is so close to the lens rim that the dashed square lies partly outside the glass, we should truncate the annular width as shown in Fig. 8(B). The area then is

$$A_G' = (\pi/4)(D_G - t_E + 2y_c)(D_G + t_E - 2y_c) . \quad (7)$$

Since the force is not uniformly distributed over either glass area, it is appropriate to use an "effective" area equal to one-half the geometric area to determine the preload, P_3, produced by the temperature change from the following equation:

$$P_3 = K_3 \Delta T \quad (8)$$

where:

$K_3 = -E_G A_G E_M A_M (\alpha_M - \alpha_G)/(2)((E_G A_G/2) + E_M A_M)$

α_G = coefficient of thermal expansion of the glass in ppm/°C

α_M = coefficient of thermal expansion of the metal in ppm/°C

and the remaining parameters are as defined above. Note that K_3 is specific to the design since it depends, in part, upon the lens and cell areas. Also, we assume the expansion coefficients to be constant over the entire temperature range of interest.

Equation (8) resembles an equation given by Bayar[10] for the stress developed in a lens as the temperature drops by ΔT. His equation applies to columns of glass and metal with equal cross-sectional areas tied together at the ends. Since the areas are not generally equal in a real design and they, as well as the lengths of the columns, do not appear in Bayar's equation, it is not an appropriate vehicle for computing the thermal preload.

The usual low temperature specification for survival of military optical instrumentation is -62°C; the corresponding value of ΔT is -82°C It should be noted that any preload, $P_1 + P_2$, existing at assembly should be added to that estimated by Eq. (8) before computing the contact stress level at the reduced temperature. This is contrary to the approach suggested by Yoder[11] in which the stresses at assembly and at low temperature were added directly.

The bulk stresses at T_{min} in the glass and in the

metal are here defined as S_{BG} and S_{BM} respectively. They can each be estimated by dividing the total preload, P_T, by $A_G/2$ (or $A_G'/2$ with a truncated stressed region) and by A_M.

3.3 Effects at Elevated Temperature

As the temperature rises, the metal of the mount expands more than the glass component within. Any axial preload existing at assembly temperature T_a (=20°C) will then be reduced. If the temperature rises sufficiently, that preload will disappear and, if not otherwise constrained (as by a sealant), the optic is free to move within the mount due to external forces. Unless the changes in position and orientation of the lens within the small axial and radial gaps created by differential expansion are smaller than the allowable motions for the application, the design should prevent such freedom at the highest temperature that the instrument is to survive without damage. Let us define this as T_C. For military applications, T_C is typically 71°C. Instruments for laboratory, commercial or consumer use may have lower survival temperature requirements. In special applications, T_C may exceed 71°C.

The axial gap developed between the cell and the lens after preload has been released can be approximated as

$$\Delta Gap_A = (\alpha_M - \alpha_G)(t_E)(T_C - T_a) \qquad (9)$$

where all terms are as defined above.

One way of preventing release of preload is to provide a preload at assembly, P_2, such that the axial force on the lens is just reduced to zero at T_C. Defining the temperature reduction from T_C to that at assembly, T_a, as ΔT, we can use Eqs. (5) through (8) and the geometry of Figs. 7 and 8 to estimate P_2. By adding P_1 and P_2 we obtain the total axial preload, P_T, required to constrain the optic against both axial acceleration forces and to prevent complete release of assembly preload at the highest temperature. Note that whenever the temperature drops below T_a, we incur additional preload (P_3) as discussed earlier.

3.4 Retaining Ring Torque Required to Produce a Given Axial Preload

The torque, Q, that should be applied to the retaining ring to introduce a given axial preload, P, to the edge of the lens can be approximated from an emperically-derived formula given by Kowalski:[12]

$$Q = 0.2 P_T D_R \qquad (10)$$

where D_R is the pitch diameter (in cm) of the thread on the ring and P_T is in N. Q is then expressed in N-cm.

3.5 Bending of the Component due to Axial Forces

If the lines of contact between the mount and optical component occur at different radii from the axis, axial forces applied through those contacts can cause bending of the surfaces. See Fig. 9. One of the surfaces must necessarily be placed in tension; this is the condition in which glass is the weakest. The following equation due to

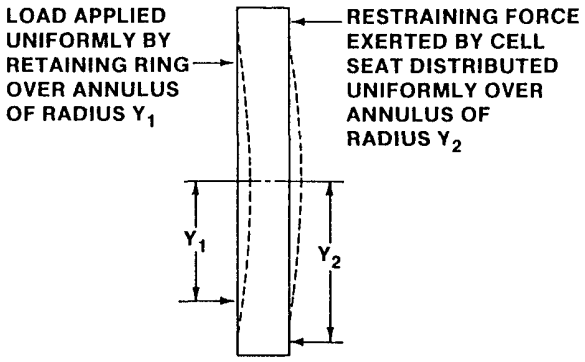

Fig. 9 - Bending forces exerted on a lens approximated by a plate of uniform thickness) when annular contacts are not at the same radial distance from the axis. From Yoder.[7]

Rourk[6] gives the tensile stress induced by bending:

$$S_T = \frac{3P_T}{2\pi m t_E^2}\left[0.5(m-1) + (m+1)\log\frac{y_2}{y_1} - (m-1)\frac{y_1^2}{y_2^2}\right] \qquad (11)$$

where:

S_T = tensile stress in the component in N/m^2
P_T = applied axial load in N
m = 1/Poisson's ratio
t_E = edge thickness of component in mm
y_1 = innermost contact radius in cm
y_2 = outermost contact radius in cm.

As mentioned earlier, the general tolerance for tensile stress is 6.9×10^6 N/m^2.

4. RADIAL EFFECTS

4.1 "Hoop" Stress at Reduced Temperature

In all designs considered above, radial clearance was assumed to exist between the optic and the mount. In some designs, this clearance is the minimum allowing assembly so, at some reduced temperature, the metal touches the rim of the optic and, at still lower temperatures, a so-called "hoop" stress develops. The magnitude of this bulk stress, S_R, for a given temperature drop, ΔT, can be estimated as[7]

$$S_R = K_4 K_5 \Delta T \qquad (12)$$

where:

$K_4 = (\alpha_M - \alpha_G)/((1/E_G)+(D_G/2E_M t_C))$

$K_5 = 1-((2\Delta_r)/(D_G \Delta T(\alpha_M - \alpha_G)))$

D_G = lens OD in mm

t_C = mount wall thickness outside the rim of the optic in mm

Δ_r = radial clearance in mm.

If Δ_r exceeds $D_G \Delta T(\alpha_M - \alpha_G)/2$, the lens will not be constrained by the cell ID and hoop stress will not develop within the temperature range ΔT due to rim contact.

4.2 Radial Stress Within the Cell Wall

As another consequence of differential contraction of the cell relative to the lens, bulk stress is built up within the metal in accordance with the equation:

$$S_M = S_R D_G / t_C \qquad (13)$$

where all terms are as defined above. With this expression, we can determine if the cell is strong enough to withstand the force exerted upon the lens without exceeding its elastic limit. If the yield strength of the metal exceeds S_M, a safety factor exists.

4.3 Combined Axial/Radial Stress at Reduced Temperatures

Bayar[10] indicated that the combined effect of axial and radial bulk stresses within the lens can be estimated as the root sum square (rss) of the orthogonal stresses. This is most significant at the worst case reduced temperature. Hence:

$$S_{rss} = (S_{BG}^2+S_R^2)^{0.5} \quad (14)$$

where all terms are as defined above. This value should be compared to the allowable compressive stress for the glass (typically $3.45X10^8$ N/m^2) to determine a safety factor for the design.

Similarly, the axial bulk stress within the metal can be combined with the radial stress in the cell as

$$S_{rss} = (S_{BM}^2+S_M^2)^{0.5}. \quad (15)$$

4.4 Stress-Induced Birefringence

The unit optical path difference (OPD/cm) for the two states of polarized light (perpendicular and parallel) due to a given amount of mechanical stress at a given temperature can be determined from:

$$OPD/cm = 10K_S S \quad (16)$$

where
OPD is in nm
K_S = stress optic coefficient of the glass in mm^2/N
S = bulk stress level in N/m^2 = S_{BG} computed with area A_G or A_G' as appropriate.

The OPD computed by Eq. (16) is that existing within the annular region shown shaded in Figs. 8(A) or 8(B) at the edge of the lens where the axial stress is concentrated. Towards the center of the aperture, the birefringence is significantly reduced. Unfortunately, no simple means to estimate its magnitude directly for a given lens configuration is currently available.

4.5 Growth of Radial Clearance at Increased Temperatures

The increase in radial clearance, ΔGap_R, between the optic and the mount due to a temperature increase of ΔT from that at assembly can be estimated by the equation:

$$\Delta Gap_R = K_6 \Delta T \quad (17)$$

where: $K_6 = (\alpha_M - \alpha_G)D_G/2$ and all other terms are as defined above.

4.6 Elastomeric Mounting

As mentioned in connection with Fig. 6, resilient

materials such as elastomers are frequently used to suspend optical components in their mounts. If the resilient layer has a particular thickness, the assembly will be athermal in the radial direction thereby resisting stress build-up due to differential expansion or contraction. This thickness is

$$t_E = (D_G/2)(\alpha_M - \alpha_G)/(\alpha_E - \alpha_M) \qquad (18)$$

where α_E is the thermal expansion coefficient of the elastomer in ppm/°C and all other terms are as defined above.

Valente and Richard[13] reported an analytical technique for estimating the decentration Δ of a lens mounted in a ring of elastomer when subjected to radial gravitational loading. Their method can be expanded to include more general radial acceleration forces resulting in the following equation:

$$\Delta = AWt_E/(\pi Rd((E_E/(1-\nu_E{}^2))+E_S)) \qquad (19)$$

where:

Δ is in mm
A = acceleration factor
W = weight of optical component in kg
t_E = thickness of elastomer layer in mm
R = optical component OD/2 in mm
d = optical component thickness in mm
E_E = Young's modulus of elastomer in N/m^2
E_S = Shear modulus of elastomer in N/m^2
ν_E = Poisson's ratio of elastomer.

The decentrations of modest sized optics corresponding to normal gravity loading are generally quite small, but will grow under shock and vibration loading. Fortunately, the resilient material will tend to restore the lens to its unstressed location and orientation when the acceleration loading dissipates.

5. MOUNTING EFFECTS UNDER OPERATING CONDITIONS

5.1 Distortions of Optical Surfaces

In the above discussions, axial forces were assumed above to be applied uniformly over a contact area on the lens. This may not be the case if the interfacing surfaces on the cell, spacer and/or retainer are not as true and smooth as the glass surfaces. In general, the glass will

contact the three highest points on the metal first and the weaker component (usually the lens) will distort under high loads until sufficient area comes into contact to establish equilibrium.

Within limits, the distorting effects of nonuniformly applied axial forces can be reduced by making the mechanical component touching the glass somewhat resilient. Some techniques for doing this are illustrated schematically in Fig. 10. Note that such flexibility introduces a spring into the design that must be taken into account in the computation of preloads and resultant axial stresses. In fact, omission of resiliency of mechanical parts such as threaded retainers is one of the reasons the above analysis of axial stress is so conservative.

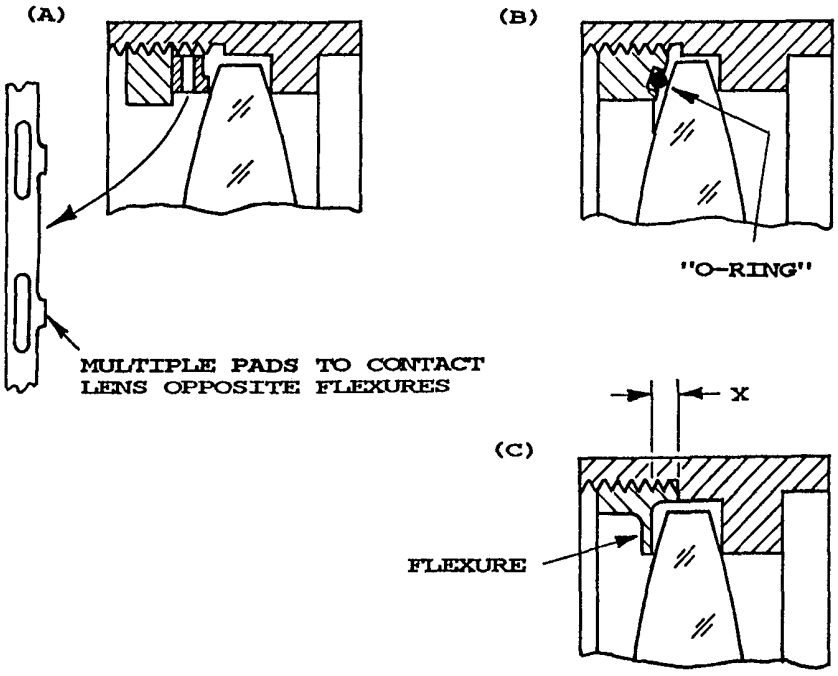

Fig. 10 - Concepts for resilient mounting interfaces to more uniformly distribute preload forces around the perimeter of a lens. From Yoder.[7]

Analytical means for predicting the surface distortions for a given optomechanical interface design, such as finite element analysis, exist. They require detailed knowledge of the shapes of the contacting surfaces and the

stiffnesses of all the optical and mechanical parts.

5.2 Stresses Under Operating Conditions

Any of the above equations for stress induced into an optical component by forces exerted by the mount can be applied to operating conditions as well as worst case conditions. In general, the stress levels will be reduced, but they still may be significant in terms of their effects upon system performance. Surface deformations due to mount-induced forces may be the worst problem, but consideration of such is beyond the scope of this paper.

6. ILLUSTRATIVE EXAMPLES

The lens mount design shown in Fig. 11 is a good example to consider here. The SK15 meniscus lens is held against a shoulder machined into an aluminum cell by a threaded retaining ring with tangent interface. The rim of the lens is ground spherical to minimize the posssibility of damage when inserted into the ID of the cell machined at assembly to clear the glass by only 0.020 mm on the diameter. Table 1 lists the design parameters of importance here.

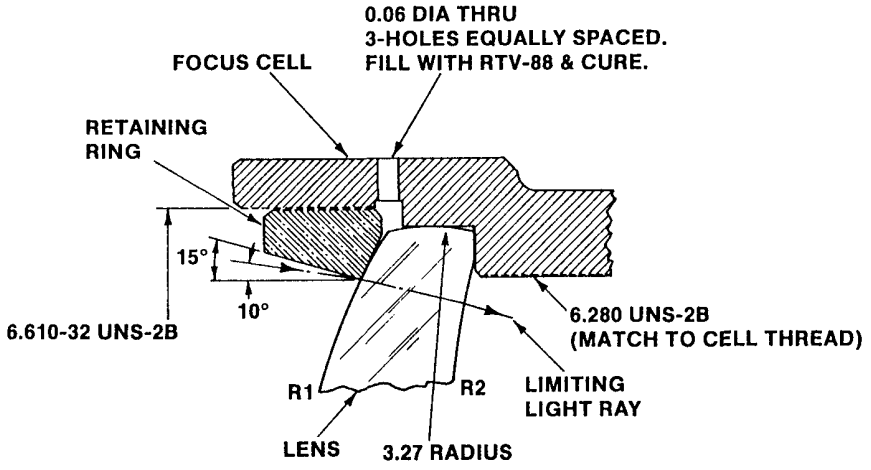

Fig. 11 - Lens mount example analyzed in the text. From Yoder.[14]

Two variations of the design have been analyzed. In the first case (see Table 2), the retainer torque is determined to give enough preload at assembly to hold the lens against 10 G acceleration as well as to clamp it at all temperatures up to 71°C. The gap that otherwise would

develop between the cell and lens at that elevated temperature is about 0.006 mm. The preload increases at a rate K_3 = 1410 N/°C so, when the temperature drops to the minimum survival value of -40°C, the preload reaches $1.57X10^5$ N. The resulting axial contact stress at T_{min} is $1.38X10^8$ N/m^2. A safety factor for the glass of 2.5 then exists.

Table 1 - Design Parameters for Example

Lens Outside Diameter (D_G)	165.9890	mm
Lens Axial Thickness (t_a)	18.9992	mm
Lens Edge Thickness @ y_c (t_E)	6.5786	mm
Surface Radius (R)	220.2180	mm
Lens Weight (W)	0.9612	kg
Cell Inside Diameter (D_M)	166.0093	mm
Cell Wall Thickness (t_c)	4.9784	mm
Interface Type	Tangent	
Glass/Metal Contact Height (y_c)	80.8673	mm
Radial Clearance (Δr)	0.0101	mm
Retainer Thread Pitch Diam. (D_t)	167.8940	mm
Max. Acceleration Factor (A)	10	G
Assembly Temperature (T_a)	20	°C
Maximum Operate Temperature (T_{maxop})	52	°C
Minimum Operate Temperature (T_{minop})	-30	°C
Maximum Survival Temperature (T_{max})	71	°C
Minimum Survival Temperature (T_{min})	-40	°C
Elevated Temp. for Contact Loss (T_c)	71	°C
Lens Material	SK15	
Poisson's Ratio (ν_G)	0.275	
Young's Modulus (E_G)	$8.41X10^{10}$	N/m^2
Coeff. Thermal Exp. (α_G)	$6.84X10^{-6}$	ppm/°C
Cell Material	Al 6061	
Poisson's Ratio (ν_M)	0.332	
Young's Modulus (E_M)	$6.83X10^{10}$	N/m^2
Coeff. Thermal Exp. (α_M)	$2.36X10^{-5}$	ppm/°C
Yield Strength	$2.55X10^8$	N/m^2
Cell Material	Ti6Al4V	
Poisson's Ratio (ν_M)	0.340	
Young's Modulus (E_M)	$1.14X10^{11}$	N/m^2
Coeff. Thermal Exp. (α_M)	$8.82X10^{-6}$	ppm/°C
Yield Strength	$6.89X10^8$	N/m^2

Using the geometry of Fig. 8(A) and data from Table 1, we compute the cross-sectional area of the stressed region within the lens and then determine the total preload and axial bulk stress within the glass for the minimum operating temperature of -30°C. Birefringence in that region of the lens is then found to be 1620 nm/cm (see Table 2).

Table 2 - Evaluation of Mounting Effects:
Case 1, Aluminum Cell and High Preload

Preload for Acceleration (P_1)	$9.43X10^1$	N
Preload for Contact @ T_c=71°C (P_2)	$7.22X10^4$	N
Total Preload @ T_a (P_1+P_2)	$7.23X10^4$	N
Retainer Torque Required (Q)	$2.43X10^5$	N-cm
Preload Increase per °C (K_3)	$-1.41X10^3$	N/°C
$\Delta T_1 = T_{min}-T_a$	-60	°C
Preload Increase @ T_{min} (P_3)	$8.46X10^4$	N
Total Preload @ T_{min} ($P_1+P_2+P_3$)	$1.57X10^5$	N
Axial Contact Stress @ T_{min} (S_A')	$1.38X10^8$	N/m²
Safety Factor for Glass	2.5	
Lens Cross Section Area (A_G)	$3.26X10^3$	mm²
$\Delta T_2 = T_{minop}-T_a$	-49	°C
Preload Increase @ T_{minop}	$6.92X10^4$	N
Total Preload @ T_{minop}	$1.41X10^5$	N
Lens Axial Bulk Stress @ T_{minop}	$8.64X10^1$	N/m²
Birefringence @ T_{minop}	$1.62X10^3$	nm/cm
Cell Cross Section Area (A_M)	$2.67X10^3$	mm²
Cell Axial Bulk Stress @ T_{min}	$5.88X10^7$	N/m²
Cell Radial Stress @ T_{min}	$1.15X10^8$	N/m²
Cell rss Stress @ T_{min}	$1.29X10^8$	N/m²
Safety Factor for Metal @ T_{min}	2.7	

At minimum survival temperature, the cell develops a bulk stress of $5.88X10^7$ n/m². Combining this on a rss basis with the radial stress generated at that temperature, we obtain the composite stress of $1.29X10^8$ N/m²; this is one-half the yield strength of the metal and therefore probably reasonable.

The main problem with this example is its great sensitivity to temperature changes. An extremely large axial preload at assembly is needed to hold the lens in place at the high survival temperature. The torque required to achieve this preload is prohibitively large. It is apparent that this design could use some refinement. One would expect the thermal problem to be reduced if the coefficient of thermal expansion of the cell were made to match that of the glass better.

In the second case evaluated, we change the cell to titanium and apply a torque to the retainer of 560 N-cm which is equivalent to 50 lb-in; a moderately heavy, but

feasible torque for this size lens assembly. Surface distortions due to mounting forces should be minimal. The mounting effects then are as listed in Table 3.

Table 3 - Evaluation of Mounting Effects:
Case 2, Titanium Cell With Reduced Preload

Retainer Torque Applied @ T_a (Q)	$5.65X10^2$ N-cm *
Resulting Preload @ T_a (P_T)	$1.68X10^2$ N
Preload Req'd for Accel. (P_1)	$9.43X10^1$ N
Preload Available to hold Contact @ T_c (P_2)	$7.40X10^1$ N
Preload Increase per °C (K_3)	$-2.05X10^2$ N/°C
$\Delta T_1 = P_2/K_3$	-0.36 °C
$T_c = T_a - \Delta T_1$	20.36 °C
$\Delta T_2 = T_{min} - T_a$	-60 °C
Preload Increase @ T_{min} (P_3)	$1.24X10^4$ N
Total Preload @ T_{min} ($P_1+P_2+P_3$)	$1.25X10^4$ N
Axial Contact Stress @ T_{min} (S_A')	$4.40X10^7$ N/m²
Safety Factor for Glass @ T_{min}	7.8
Lens Cross Section Area (A_G)	$3.26X10^3$ mm²
$\Delta T_3 = T_{minop} - T_a$	-50 °C
Preload Increase @ T_{minop}	$1.01X10^4$ N
Total Preload @ T_{minop}	$1.02X10^4$ N
Lens Axial Bulk Stress @ T_{minop}	$6.26X10^6$ N/m²
Birefringence @ T_{minop}	$1.16X10^2$ nm/cm
Cell Cross Section Area (A_M)	$2.67X10^3$ mm²
Cell Axial Bulk Stress @ T_{min}	$3.97X10^6$ N/m²
Cell Radial Stress @ T_{min}	none
Cell rss Stress @ T_{min}	$3.97X10^6$ N/m²
Safety Factor for Metal @ T_{min}	87

* Equivalent to 50 lb-in.

The rate of increase in preload with temperature (K_3) is now $2.05X10^2$ N/°C; almost 7 times less sensitive than with the aluminum cell. After allocating preload to withstand acceleration at T_a, we have practically none left to combat cell expansion under temperature rise so T_c is only 21.36°C. The contact stress at the minimum survival temperature is reduced to $4.40X10^7$ N/m² so the safety factor for the glass is 7.8. The birefringence at minimum operating temperature is reduced by a factor of about 7 from that for Case 1 to 116 nm/cm. No radial stress due to rim compression occurs at the low survival temperature so the safety factor for the cell is large (87). The thickness of the cell wall might well be reduced in this case.

Since the thermal expansion properties are fairly well matched in this design, the axial and radial gaps at maximum survival temperature (71°C) are very small. Gap_A is 0.7 μm while Gap_R is increased from 0.020 mm to 0.028 mm. The uncertainties in lens location and orientation due to these clearances are quite acceptable for the particular design investigated here. Injection of an elastomeric sealant around the rim of the lens would tend to hold the lens in place at elevated temperatures. One of several radially-directed holes provided for this purpose is shown in Fig. 11.

7. CONCLUSIONS

We have described here an approach to making engineering estimates of various mounting interface effects upon optical components such as lenses due to assembly preload and some environmental conditions. For simplicity, the equations given here do not include the effects of shear forces within materials or the inherent flexibility of mount components other than the mount (cell) wall. Omission of factors such as these cause the results to be conservative, i.e., to overestimate the magnitudes of the mounting effects. The degree of overestimation has not yet been determined. Further studies comparing results obtained by the methods outlined here to those obtained by more precise methods such as finite element analysis would help quantify this conservatism.

8. REFERENCES

1. Willey, R.R., "Maximizing both production yield and performance in optical instruments through effective design and tolerancing", Proc. SPIE CR43 (1992).

2. Shand, E.B., Glass Engineering Handbook, 3rd. Ed, McGraw-Hill, New York (1958).

3. Delgado R.B. and Hallinan, M., "Mounting of lens elements", Opt. Eng 14, S-11 (1975).

4. Hopkins, R.E., "Lens Mounting and Centering", Chapter 2 in Applied Optics and Optical Engineering, Vol VIII, R.R. Shannon and J.C. Wyant, eds., Academic Press, New York (1980).

5. Yoder, P.R. Jr., "Axial stresses with toroidal lens-to-mount interfaces", Proc. SPIE 1533, 2 (1991).

6. Rourk, R.J., Formulas for Stress and Strain, Table XIV, McGraw-Hill, New York (1954).

7. Yoder, P.R., Jr., Opto-Mechanical Systems Design, 2nd. Edition, Marcel Dekker, New York (in press, 1992).

8. Hatheway, A.E., private communication (1992).

9. Richard, R.M., private communication (1992).

10. Bayer, M., "Lens barrel optomechanical design principles", Opt. Eng. 20, 181 (1981).

11. Yoder, P.R. Jr., "Lens mounting techniques", Proc. SPIE 389, 2 (1983).

12. Kowalskie, B.J., "A Users Guide to Designing and Mounting Lenses", Digest of Papers, OSA Workshop on Optical Fabrication and Testing, North Falmouth (1980).

13. Valente, T.M. and Richard, R.M., "Analysis of elastomer lens mountings", Proc. SPIE 1533, 21 (1991).

14. Yoder, P.R., Jr., "Opto-mechanical designs for two special-purpose objective lens assemblies", Proc. SPIE 656, 225 (1986).